Targeting of single stranded oligonucleotides through metal-induced cyclization of short complementary strands

Fabrice Freville, Tristan Richard, Katell Bathany, Serge Moreau

Targeting of single stranded oligonucleotides through metal-induced cyclization of short complementary strands

by **Fabrice Freville**[a], **Tristan Richard**[a], **Katell Bathany**[b] **and Serge Moreau**[*a]

[a]INSERM U386, Bordeaux, Université Victor Segalen Bordeaux2, 146 rue Léo Saignat F-33076 Bordeaux Cedex, France

[b]Institut Européen de Chimie et de Biologie (IECB), 2 rue Robert Escarpit, 33607 Pessac Cedex, France

* serge.moreau@bordeaux.inserm.fr

Abstract

A new strategy to cyclize a short synthetic oligonucleotide on a DNA or a RNA target strand is described. The approach is based on metal-templated cyclization of short synthetic oligonucleotides conjugated with two chelating 2,2':6',2”-terpyridine moieties at their 3' and 5' ends. Cyclization following metal addition (Zn^{2+}, Fe^{2+}) was demonstrated by means of thermal denaturation experiments, MALDI-Q-TOF6MS and gel electrophoresis (PAGE). 1D- and 2D-NMR experiments were performed to analyse the association of complementary strands after metal-mediated cyclization. Our protocol allows the efficient circularisation of synthetic oligonucleotides. Thereby, the hybridization on a complementary strand was more efficient with a RNA target strand and a 2'-O-methyl circularized oligomer.

Introduction

RNA can form stable structures with a small number of nucleotides. Combination of various secondary structural elements can lead to tertiary structures of increasing complexity [1]. Such structures are involved in numerous regulation processes through interactions with RNA, DNA or proteins [2]. The iron-responsive element (IRE), a hairpin structure present in mRNAs coding for key proteins in the iron metabolism of vertebrate cells, is a good example [3]. Numerous examples of functional RNAs are also found in viruses, TAR RNA is the RNA sequence required for transactivation of the of the transcription of the HIV-1 genome [4]. So ligands designed to target such RNA motifs may allow the control of the metabolic processes that they mediate.

We are interested in strategies aiming at locking, through catenane formation, synthetic oligonucleotides on hairpin motifs of RNA an essential secondary structure of RNA often involved in regulation of gene expression [3]. Catenanes are intertwined polymember rings tied together [5, 6]. Such bulky synthetic complexes on RNA hairpin may allow an efficient inhibition of the association of the natural ligands of these structures. Our first attempt in this line is developed here using modified oligonucleotides bearing terminal 2,2':6',2”-terpyridines moieties which may lead, following addition of metal ions to the formation of a catenane structure with the targeted hairpin (Scheme 1A). Cyclic,[7] polymeric [8] and chiral assemblies [9] could be obtained utilizing the chemistry of terpyridines and metal complexes. Physiologically available ions such as zinc could be recruited to mediate such a process [10]. The high dynamic characteristics of Zn-$(Tpy)_2$ complexes will allow an easy closing of the ligand on a RNA hairpin [11]. We previously developed methods of conjugation of terminal terpyridine (Tpy) on synthetic oligomers and showed that metallic coordination lead to large

increase in the stability of duplexes or short hairpins [12]. In order to evaluate the ability of terpyridine modified oligonucleotides to cyclize around the targeted strand we designed a simplified system where the target strand (DNA or RNA) is a short linear sequence allowing the formation of a 9 base pair duplex with the Tpy-modified oligomer. Such a one turn helical duplex will put the 3' and 5' Tpy residues in a face-to-face conformation allowing an easy closing through metal coordination and leading to a target strand passing through the circularized Tpy oligomer (Scheme 1B). This topology is a prerequisite for the formation of the interlocked rings of a catenane structure.

The target oligomer sequences were derived from a RNA hairpin of the internal ribosomal entry site (IRES) of the hepatitis C virus (HCV). The apical loop of the domain IIIb of this IRES fulfil some of the above mentioned criteria. First it is involved in the IRES function by recruiting essential co-factors of translation initiation such as eIF3 [13]. Second the length of the loop (14 nt) allows the hybridization of a complementary strand leading to a one turn helical double helices.

Results

Oligomers sequences.

All strand sequences are shown in Table 1. Either DNA or RNA sequences were used as targets. The complementary strands were DNA and 2'-O-methyl oligonucleotides. Analytical data of chemically modified oligomers are reported in Table 1.

Molecular modeling and chemical synthesis.

We chose a new chemical approach we used recently to allow an easy synthesis of bis-terpyridine conjugated oligonucleotides. [14] This one relies on the use of 2,4-

dihydrobutyramide as substitute for nucleosides as shown by Dioubankova.[15] This synthon allows the introduction of various ligands or labels at both ends of oligonucleotides through phosphoramidite chemistry and the synthesis of specific solid support. To define the length of the chemical link between the Tpy moieties and the 3', 5' OH groups of the cyclic oligomer according to scheme 1, we built an initial duplex using an ideal A-form double-helical model. The coordination link and geometry of the terpyridines units were constrained according to coordinate data of X-ray diffraction study of iron complexes [16]. The general structure of Tpy conjugated oligomers are shown in scheme 2A. A representation of the optimized structure of the hybridized A -form duplex is depicted in scheme 2B.

Melting temperature experiments.

As a first analysis of the putative circularization of the Tpy-modified oligomer around its target, we designed various combinations of complementary strands and followed their association by UV monitored thermal denaturation experiments. Three kinds of duplexes were used: type 0 for unconjugated oligomers, type I for mono-terpyridine conjugates and II for the bis-terpyridine ones. Strands associations were studied in metal free buffer (10 mM phosphate buffer (pH 7.0), 150 mM sodium chloride, 200 µM EDTA) and in the presence of control amounts of metal ions (Zn^{2+}, Fe^{2+} , Ni^{2+}) using the same buffer without EDTA. Added equivalents refer to the duplex concentration (1µM). The experimental data for DNA targets are reported in Table 2. Denaturation of the samples were carried out by increasing the temperature from 4°C to 90°c. The melting temperature was obtained through graphical methods. Tm uncertainty obtained from multiple experiments are ± 1°C. A striking feature of these data are that type II duplexes exhibited a significant drop in Tm values compared to any other strand associations. Although Tm data were difficult to determine in these cases, a melting transition

(Tm values around 10 to 20°C) with a significant hyperchromic effect can be seen on heating such samples. Figure 1 shows typical transition of duplexes **0a** and **IIa** in the presence of one equivalent of Zn^{2+} ion. Type II duplexes are clearly formed at low temperature. As a comparison a mismatch duplex (**0b**, Table 2) was checked and failed to show a melting transition. Type 0 duplexes showed expected Tm values both in metal free buffer or with added metal ions with slight variations around 29.0 °C. The Tm of type I duplexes (one strand with one Tpy moiety) are rather insensitive to metal addition. A slight contribution of the terpyridine to the stability of the duplexes was detected even in metal free buffer. Such a behaviour as already been reported [12]. Thus the specific behaviour of type II duplexes is related to the presence of the two Tpy moieties at both 3' and 5' ends of one strand. Extension of the link between the two conjugated Tpy by intercalation of one or two unpaired T nucleobase did not result in a different behaviour (compare data **IIa** to **IIb** and **IIc** in Table 2). In order to take into account the potential effect of dangling nucleotides of the target strand 1, when hybridized to its complementary oligomer, we studied various duplexes including a shorter target strand allowing the formation of blunt ends duplexes (Strand 2, Table1). As revealed in Table 2, these new duplexes (**0c**, **Ic**,**d**, **IId**,**e**,**f**) exhibited very similar behaviour to the one observed for duplexes **Ia** through **IIc** (Table 2). Type II duplexes, always revealed Tm between 10 to 20°C. Thus dangling ends of the target cannot be responsible for these specific Tm drops.

Metalation of the bis-Tpy strand **7**, **8** or **9** is associated with the drop in Tm values. This suggested to us that the link between the two Tpy units through metal complexation was involved in this behaviour. We then added excess of metal species in order to promote the formation of mono-metalated entities and thus disrupt the coordination link between the two nearby Tpy. Such a goal can be easily achieved through slight excess of Ni^{2+} ions or larger amounts of Zn^{2+} ions [12, 17]. Data in Table 2 showed that 2/1 (Ni^{2+}/duplex) ratio or 20/1

(Zn^{2+}/duplex) led to significant increase in Tm values of duplexes **IIa** to **IIf** (28.3 to 42.4 °C) in comparison with 1/1 metal to duplex mixture (<20°C). Even in large excess, Fe^{2+} ions failed to promote the formation of mono-metalated Tpy as predicted from thermodynamics and kinetics data [11, 17].

We extended this study to RNA targets and 2'-O-methyl ligands. Data are gathered in Table 3. As expected for such strands combinations we observed a raise in Tm values compared to those of similar duplexes in Table 2. Thus the unmodified **0r** duplex exhibited a melting temperature of 40.4°C, 11.5 °C higher than that of the corresponding duplex **0a**. Type II duplexes exhibited cooperative melting transitions allowing the determination of Tm in this case. However we always noticed a drop in Tm of these duplexes (close to 10°C) compared to those of type 0 and I duplexes upon addition of 1 equivalent of metal ion. (Table 3, columns 4 and 5). Slight excess of Ni^{2+} ion (2/1 metal/duplex) led also to an increase in Tm revealing the disruption of the coordination link between the two Tpy moieties (column 7). A noticeable difference between DNA and RNA strands was that extension of the link between the Tpy units allowed in this last case an increase in Tm. Insertion of one or two unpaired T nucleobases in the target strand also increased Tm from 29.9 to 37.3°C (Table 3, duplexes **IIrb** and **IIrc**, columns 4,5). An interesting observation was linked to the addition of Mg^{2+} ions on type **IIr** duplexes. In these cases Tm values observed for bis-Tpy-modified oligomers reached and in some cases exceeded those determined for the unmodified duplex **0r** (Table 3, column 8,9). Thus, the duplex **IIrc** composed of the RNA strand **1r** and the extended 2'-O-methyl (**9m**), melted at 46.6°C, 4.8°C higher than the corresponding unmodified duplex **Ir** (41.8°C) in the same experimental condition (see Table 3, column 9). At physiologically relevant Mg^{2+} concentration (3mM), the increase of Tm is 2.4°C (Table 3, column 8).

Mass spectral analysis.

The stoichiometry of various metal complexes was studied using mass spectrometry. Prior to mass spectral measurements, single-stranded or double-stranded oligomers were metalated using the same experimental conditions as the one used for thermal denaturation experiments i.e concentration, buffer, pH (see experimental protocols). An aliquot was then sampled and the buffer was exchanged for ammonium acetate.

Data for MS analysis are gathered in Table 4. The mono-Tpy conjugated strands **5** was analysed first by MALDI-Q-TOF MS. Before metalation, a mono-isotopic peak at m/z 3361.75 was observed (Calcd. for $[M-H]^-$, 3361.75). After metalation with Fe(II) ions, at a ratio of 1/1 metal to oligomer, the formation of a 2/1 complex between **5** and Fe(II) was demonstrated through the presence of peaks at m/z 6778.27 (Calcd. for $[2M+Fe-3H]^-$, 6778.34) and m/z 3388.60 (major peak of the spectrum, calcd. for $[2M+Fe-4H]^{2-}$, 3388.67). Similar results were observed for strands **5m** (the corresponding 2'-O-methyl derivative of 5) with detection of peaks at m/z 7318.55 and 3658.79 corresponding to the $[2M+Fe-3H]^-$ and $[2M+Fe-4H]^{2-}$ species respectively (calcd. for $[2M+Fe-3H]^-$, 7318.61).

We then studied the bis-Tpy conjugates **7** and **7m**. As expected the non-metalated species were characterized by mono-isotopic peaks at m/z 3944.95 (Calcd. for $[M-H]^-$, 3944.98) and at m/z 4215.09 (Calcd. for $[M-H]^-$, 4215.07). Metal complexation was then performed by incubation of single-stranded species with Fe^{2+} ions at ratio of 1/1 to 2/1 metal to strands. The same results were obtained for these 2 stoichiometric conditions. The spectrum is shown in Figure 2. A mono-isotopic peak at m/z 3998.91 was observed for strand **7** (Calcd. 3998.89 for $[M+Fe-3H]^-$) and m/z 4268.99 (Calcd. 4268.98 for $[M+Fe-3H]^-$) for strand **7m**. We thus only revealed the 1/1 complex between bis-Tpy conjugated strands and Fe^{2+} ions. In order to check

for the presence of higher oligomeric species the same experiment was performed using MALDI-TOF MS which allow higher m/z analysis (up to 10 000). Fe^{2+} or Zn^{2+} ions were added to strand **7** at ratio of 2/1 (metal/strand). 1/1 complex were characterized in each cases at m/z 4001.9 for $[M+Fe-3H]^-$ and m/z 4010.8 for $[M+Zn-3H]^-$ with calculated data of 4000.8 and 4010.4 respectively. We never observed peaks at higher m/z. However following incubation of Zn^{2+} ions at a ratio of 2/1 metal to strand we observed a small peak at m/z 4073.4 corresponding to a bis-metallated species (Calcd.for $[M+2Zn-5H]^-$, 4073.8)

We have next investigated double-stranded complexes (Table 4). We chose to study the Zn^{2+} metalated species. For MALDI-Q-TOF MS analysis, the complex **IId**, were annealed in the same conditions as those used for Tm measurements (ratio 1/1, metal/duplex). The main peak at m/z 2653.45 corresponds to the target strand **2** (Calcd. for $[M-H]^-$, 2653.46). Two minor peaks were detected at m/z 4006.87 and 4068.79 corresponding to the bis-Tpy oligomers $[M+Zn-3H]^-$ and $[M+2Zn-5H]^-$. The full complex **IId** was also detected as a minor peak at m/z 6666.00 (Calcd. for M_{IId} +Zn-3H]$^-$, 6666.08). The same experiment has been performed with complex **IId** annealed in the presence of an excess of Ni^{2+} ions (2/1; metal/duplex ratio). As already observed, the main isotopic peak at m/z 2653.46 corresponds to strand **2**. We noticed a clear increase in the intensity of isotopic peaks at 4000.87 and 4056.81 which corresponds to $[M_7+Ni-3H]^-$ and $[M_7+2Ni-5H]^{2-}$ respectively (Calcd. 4000.89 and 4056.81). Very weak peaks were detected at m/z 6659 and 6716 which correspond to the occurrence of the complexes $[M_{IId}+Ni-3H]^-$ $[M_{IId}+2Ni-5H]^-$ (Calcd. 6659.44, 6716.11). Non-metalated species could not be detected.

Gel shift analysis

Gel shift analysis by PAGE was used to characterize the molecular species involved in

the type II duplexes. Figure 3A shows the PAGE analysis of single strands (**1r**, **3m**, **5m**, **7m**) incubated in metal free conditions (EDTA completed buffer) or with Fe^{2+} ions before loading on the gel. Lanes 1, 2, 3 and 6 correspond to unmetalated species. 1 and 6 are respectively the target RNA strand (13 nucleotides) and the unconjugated 2'-O-methyl complementary strand (9 nucleotides). 2 and 3 correspond to the mono and bis Tpy conjugated strands. They are separated according to their molecular weight. Lane 4 and 5 shows the band shifts observed upon incubation of one equivalent of Fe^{2+} ions with each strand **7m** and **5m** respectively. The slowest moving band (lane 5) corresponds to the mono-Tpy conjugate as expected for an intermolecular complex "Fe^{2+}(**5**)$_2$" with a double chain length. In contrast a fast moving band (lane 4) was observed for the bis-Tpy conjugate **7m** when metalated with Fe^{2+} with a mobility close to that of the unmetalated strand **7m**. Iron(II) Tpy complexes were easily detected on the same gels thanks to their highly coloured (purple) octahedral complexes (Figure 3B) were lane numbers 1', 2', 3', 4', 5', 6' correspond to the same samples as figure 3A visualized under day-light. A faint spot is observed for lane 5' apparently due to diffusion as observed for lane **5**. Both the monomeric nature and the metalation of the molecular species of the spot (lane 4) were confirmed by elution and MALDI-Q-TOF analysis (m/z: 4268.99). Elution of the band on lane 5 confirmed the high molecular weight of the complex "Fe^{2+}(**5**)$_2$" (m/z 7318.55 and m/z 3658.79). Similar results were obtained with DNA strands **1**, **5**, **7** (data not shown).

NMR experiments.

We report here some preliminary NMR analysis of various duplexes. We chose duplex **0a**, Ia and **IIa** in order to carefully measure the impact of Tpy conjugates on theses double-stranded structures. Unmetalated duplexes **Ia** and **IIa** were compared to the metalated ones.

Samples were prepared on a 0.8 mM scale, one and two-dimensional spectra were acquired in H_2O/D_2O (90:10) with 10Mm phosphate buffer, pH 7,0 at 277°K. When needed Zn^{2+} ions were added stepwise until the stoichiometry of one metal for two Tpy ligands was reached. Our first analysis relies on the imino protons regions of the spectra. The imino resonances of the duplexes were assigned primarily from the imino-imino crosspeaks in the 2D NOESY spectra. Figure 4 shows the exchangeable imino region (11-15 ppm) of the one-dimensional 1H NMR spectrum for the three studied duplexes in metal free conditions or after Zn^{2+} ions complexation.

Duplex **0a**. Base pairs are numbered according to Figure 4. Imino protons are then numbered according to base pairs number, thus as an example, $G2N_1H$ and $T4N_3H$ imino protons are abbreviated here as G_2 and T_4. All expected base pairs were detected on the duplex as deduced from the peaks found on Figure 4A. Imino-imino NOE cross-signals occured sequentially and allow the assignment of all imino protons. The imino-proton of G_2 base pair which resonates at 12.09 ppm served as a starting point for the assignment (Figure 5). A clear overlap was observed for T_3 and T_8. As a result of exchange with the solvent, cross-peaks of G_1 and G_9 are absent in the 2D NOESY spectrum, and the resonance of these last protons exhibit a significant broadening compared to other imino peaks but are however clearly detected. Chemical shifts data are gathered in Table 5. (G_1 and G_9 assignments are reversible).

Duplex **Ia**. In the duplex Ia, which includes a 3' Tpy ligand on the shorter strand 5 (Table 1), the guanine resonances are clearly affected and significantly broaden (Figure 4B). G_1, G_9 and G_2 lines could not be assigned, exhibiting significant larger line-widths. On the opposite the central G_6 resonance was not perturbated . The thymine imino region of the spectrum was also affected. The imino resonances of base pairs 3 and 4, localized in the vicinity of the Tpy conjugate, are broaden. Base pairs located at the opposite duplex end, T_7 and T_8 are not perturbated , T_5 line being slightly broadened. As is evident in Table 5, some resonances are

also shifted in comparison with that of duplex **0a**. These variations in chemical shifts correlates with the variations in line-width. The observed upfield shifts of imino protons decrease from G2 to T5, ranging from 0.26 to 0.05 ppm.

Duplex **IIa**. The NMR 1D spectra of duplex IIa shows only 5 resonance lines (Figure 4C). They are all located on the 5' end of the bis-Tpy conjugated oligomer (strand 7, Table 1). Surprisingly the terminal G_9 base pair is easily detected and exhibited a sharp resonance. G6 resonance line is not perturbated and exhibit similar characteristics in the three duplex (**0a**, **Ia**, **IIa**) both in line-width and chemical shifts (Table 5). Among the five expected lines of thymine base pairs, only 3 are detected (T_5, T_7, T_8). T_5 and T_7 are slightly broadened (compared to **Ia**, Figure 4B). The comparison of their chemical shifts between duplex **0a** and **IIa** reveal also an upfield shift of resonances closed to the 5' Tpy ligand, ranging from 0.3 to 0.07 ppm. The shift regularly decrease from the 5' end to the core of the duplex.

We have then study the metalated duplexes Ia and **IIa** after addition of one Zn^{2+} ions for two Tpy ligands. The 1D spectra are shown in Figure 4D and 4E. We first studied the impact of metalation on the mono-Tpy conjugated duplex **Ia**. In these experimental conditions an intermolecular metal complex between two duplexes is expected. The observed pattern for imino resonances was closed to the one observed for the unmetalated spectra (compare Figure 4B and 4D). The main features of theses data, were the sharper resonance lines for T_3, T_4 and T_5 and their minor variations in chemical shifts (Table 5) compared to unmetalated duplex **Ia**.

The NMR imino region of the metalated duplex **IIa** is shown in Figure 4E. Compared to duplex **IIa** (Figure 4C) much more resonance lines are observed both in the guanine and the thymine imino region. This might be due to an equilibrium between two or more structures in the NMR sample. We assigned five main resonances which we supposed to belong to the major

component of the mixture. The resonances we observed (G_2, T_3, T_4, T_5, G_6) are located on the 3' end of the bis-Tpy conjugated strands, and the observed chemical shifts are closed to those observed for the unmodified duplex **0a**. The metalation of duplex **IIa** was checked by mass spectral analysis. An aliquot of the NMR sample was submitted to MALDI-TOF (negative mode) and lead to a major peak at m/z 4010.4 (calcd. for [M+Zn-3H]$^-$, 4010.40] in full concordance with a mono metalated bis-Tpy conjugate.

Discussion

We previously demonstrated that the high affinity metal chelator Tpy [17] could be used to assemble and stabilize two complementary oligonucleotides [12, 14]. The conjugation of Tpy moieties to stem-loop oligomers provided an efficient procedure for the cyclization of the oligomer after addition of metal ions. We report here an extension of these concepts by studying the potential of 3',5' Tpy conjugated oligonucleotides to wrap round a complementary strand when linked through metal coordination. In order to allow such a cyclization, we conceived specific linkers between the Tpy moiety and the terminal OH groups of oligonucleotides. These linkers were optimized through modeling. As shown in scheme 1B a one turn helical duplex will put the Tpy ligand in a face-to-face position, which when coordinated to a metal ion lead to a circularized oligonucleotide where the complementary strand passes through this circle. This topology is a prerequisite for the formation of a catenane when the target strand is also a circular oligonucleotide. In a recent paper by Göritz and Kramer a complementary approach was developed [18]. A bis-Tpy conjugated DNA strand was circularized through metal chelation, such as conformational restrictions unable double helix formation. The complementary sequences they used involved the formation of 15 base pairs

duplex. This corresponds to a one and a half double helix turn, which put the Tpy moieties at opposite positions along the duplex. The short and non optimized arms they used for the links between 3' and 5' terminus of the bis Tpy conjugated strands will not favour the chelation of the Tpy units when hybridized to the complementary sequence.

We designed here a simplified system in order to check the conformational restrictions of such a topological object. We chose to explore the two main helical forms of nucleic acid helices by studying both B DNA duplexes and the A RNA conformation of a RNA 2'O-Me hybrid [19]. The 9-base pairs model we chose was derived from an apical loop from HCV genome. It fulfils the above criteria i.e. a length close to a one turn double-helical duplex. We have then analysed the molecular species involved in the metalated duplexes through various techniques.

Mass spectral analysis allowed us to show that the species resulting from metal addition to the bis Tpy-conjugated single strands **7** and **7m** were a 1:1 complexes between metal and the oligomer (See Table 4). This well defined stoichiometriy could account for either a monomeric (1+1) intramolecular metallo-macrocycle or oligomeric (n+n) species. As we could not detected higher molecular weight entities by mass spectral analysis we tried to confirm the molecular size of the metallic complex using gel shift analysis in denaturating conditions. The mobility of the band in lane 4 (Figure 3A) is in full concordance with a low molecular monomeric compound, metalation being easily detected both by the high coloured band in Figure (lane 4, Figure 3B) and by mass spectral analysis after elution of the spot. Taken together these data lead us to conclude that **7** and **7m** strands are fully circularized in the experimental conditions used here. Although our experimental data do not discard the simultaneous occurrence of a monocomplex terpyridine and an unmetalated one, the thermodynamic data do not favour this possibility, particularly for iron(II) complexes [17]

Melting experiments allowed us to analyse the response of the circularized oligomer when annealed to its complementary strand. Data obtained from DNA duplexes (Table 2) underline a specific behaviour of the bis Tpy-conjugated oligomer when incubated with their target strand in the presence of metallic ions. At low temperature circularized Tpy-oligomers are paired to their targets. The observed destabilization of these duplexes (**IIa**) in comparison with unmodified duplexes **0a** or mono-conjugated oligomer (**Ia**) is correlated with the occurrence of the coordination link between the two terminal terpyridines moieties. The released of this constraint by disruption of the link between the two Tpy (by addition of a slight excess of Ni^{2+} ions) is associated with a raise in melting temperature that reach those observed for unconjugated or metal-free duplexes. We thus concluded that the circularized metalated oligomer is annealed to its complementary strand. Furthermore the 2'-O-methyl circularized oligomer was able to anneal to its targeted RNA strand and reach melting temperature close to that of unmodified duplexes (Table 3). This was observed first by adding magnesium to the incubation medium. The magnesium dependence of RNA folding and RNA strand association is well documented [20, 21]. We never observed such a dependence for DNA duplexes (**IIa** through **IIc**, data not shown). When we tried to release putative conformational constraints by inclusion of unpaired nucleotides (T or U) at one or the both ends of strands **8m** and **9m**, the corresponding duplexes (**IIrb**, **IIrc**) melted at higher temperatures following metal addition (Table 3, column 4 and 5). Such an effect was not observed for duplexes **IIb** and **IIc**. Additive effects are observed following magnesium addition to these extended strands. These both effects suggest that the conception and design of the link between the Tpy moieties and the oligonucleotides deserve more studies.

Duplex formation on circularized oligomer (**7**) was clearly shown also by NMR. Base pairs are easily detected through imino proton resonances in NMR experiments in the range 11-

16 ppm [22]. As shown in Figure 4 at low temperature (0°C) the duplex **IIa** revealed the occurrence of at least 5 imino proton lines in the range 11 to 14 ppm. It also lead us to suggest that mixtures of closely related helical conformers are formed after metal addition to duplex **IIa**. This observation precluded to further analyse the structure of the complex between the annealed strands by NMR. We are thus unable to conclude on the topology resulting from their association and if scheme 2B provides a realistic representation of the structure.

NMR data revealed also some interesting experimental observations. According to melting temperature experiments, 3' or (and) 5' conjugation of Tpy units resulted (in the absence of metal ions) in slight increases in Tm of the corresponding duplexes (Table 2). 5' conjugation is generally more efficient in this stabilization as already observed [14]. NMR data showed an increase in the dynamic of base pairs located close to the 3' conjugation and on the opposite an increase in the life time of base pairs located on the 5' side. On both ends of duplex **IIa** an upfield shift of imino protons was observed compared to **0a**. These observations suggest a different mode of interaction of Tpy with the double strand when located at the 3' or 5' end, correlating with differences in the stabilization abilities of these conjugates. Although the upfield shifts of imino protons following conjugation of Tpy suggest an intercalative mode of binding [23], we never noticed clear stabilizing properties of free Tpy ligands for double-stranded DNA [12]. A partial dynamic intercalation of the unmetalated Tpy could account for the observed dynamic of 3' base pairs. A 5' stacking of the 5' Tpy on the last base pair could contribute to the sharper resonance observed for imino proton G9 on the duplex **IIa**. However an interaction of both Tpy within the minor or major groves could also not be excluded [24]. Only a complete structural analysis of such a duplex will allow a more comprehensive understanding of these experimental data.

In conclusion, in this report we have shown that a short synthetic single stranded

oligonucleotide bearing terminal terpyridines is easily cyclized through metalation. It can be used to target DNA or RNA strands. Our study underline that the link between the Tpy moieties and the 3',5' ends of oligomers have to be carefully designed to allow a thermodynamically favorable association between strands after metalation. More studies have to be conducted to design new links according both the nature of the targeted strand and the chemistry of the synthetic circular strand. In this last objective, 2'-O-methylated RNA seems to be the most promising approach to design efficient circularligands for RNA.

Experimental Part

Oligonucleotides synthesis

Unmodified oligonucleotides were purchased from Eurogentec. All modified oligonucleotides were synthesized on a 0.2 µmol scale on a Millipore expedite 8909 DNA synthesizer using conventional ß-cyano-ethyl phosphoramidite chemistry. The modified and standard bases were dissolved in anhydrous acetonitrile (0.1M final concentration). The modified phosporamidites were coupled manually with a coupling time of 15 min. The coupling efficiency was the same as that of unmodified amidites. All oligomers were synthesized "trityl off". Standard deprotection procedures were used according to DNA and RNA sequences. The crude oligonucleotides were purified by electrophoresis on denaturating (20%) poyacrylamide gels. The pure sample were desalted through reverse-phase maxi-clean cartridges (C18, Altech).

UV thermal melting experiments

Purified oligonucleotides (each strand 1 µM) were diluted in 0.5 ml of the appropriate buffer : 10 mM phosphate buffer (pH 7) 150 mM NaCl, 100 µM EDTA for metal free

experiments. Other experiments were performed with the same buffer without EDTA. Metal addition was carried out by adding aliquots of the metal salt solution. The mixtures were boiled for 2 min and the hybridization was assured by a low-temperature cooling of the sample. Melting experiments were performed with a Cary 1E UV/Vis spectrophotometer with a temperature controller units. Samples were kept at 4°C for at least 30 min and then heated from 4 to 90°C at a rate of 0.4°C/min. The absorbance at 260 nm was measured every 30 s. The melting temperature was determined using graphical methods [4] and reported data are the mean from at least three experiments.

Mass spectral analysis.

MALDI-Q-TOF mass spectrometry were performed on a Waters Ultima spectrometer for negative-ion detection using reference oligonucleotides for mass calibration allowing a mass accuracy better than 0.01 Da. A special preparation technique was designed to analyse Tpy-modified oligonucleotides. the stainless-steel target was first covered with a thin layer of matrix [0.5 µl of 2,4,6-trihydroxyacetophenone (THAP) 10 mg/ml in acetone] and this layer was washed with standard EDTA solution (2 x 1 µl) and water (2 x 1 µl). The oligonucleotides (0.8 µl of 20 µM solutions in water) were then deposited on this matrix layer and allowed to dry. The final preparation step was the application of a second layer of matrix [0.8 ml of a 4:1 solution of THAP (10 mg/ml in ethanol) and 100 mM aqueous ammonium citrate] and drying at room temperature.

MALDI-TOF measurements were performed with a Bruker Reflex III instrument. The same sample preparation as mentioned above was used for all Tpy-conjugated oligonucleotides.

Gel shift assay

The gel shift analysis were performed in denaturating 20% polyacrylamide using tris buffer pH 8.4. The electrophoresis was carried out at 200 or 150 V at 4°C. Gels bands were revealed by UV-shadow, or visualized by day-light for highly coloured terpyridine iron complexes.

NMR spectroscopy.

NMR experiments were performed on a 500 MHz Bruker Avance spectrometer with a z-gradient TXI probe. Samples were prepared on a 0.8 mM scale, one and two-dimensional spectra were acquired in H_2O/D_2O (90:10). The pH of all the solutions was set to 7.0 with a 10 mM sodium phosphate buffer. When needed Zn^{2+} ions were added stepwise until the stoichiometry of 1:2 (metal/Tpy) was reached. The 1D and 2D spectra were recorded at 273K. The 2D spectra of the imino region were performed with 300 ms mixing times. A combination of Watergate and Jump and Return sequences was used for water suppression [25]. Proton chemical shifts were calibrated against TSP (trimethylsilylpropionic acid). All spectra were collected in a phase sensitive mode via STATES-TPPI method and processed according, by using TOPSPIN software.

Structure calculations

Energy minimization was used to optimize the Tpy-modified oligomer for wrapping the Tpy-modified oligomer ligand round the targeted strand. The structure calculations were performed on a Silicon Graphics Fuel workstation using the DISCOVER module of INSIGHTII program (Accelrys), applying CVFF forcefield. The initial complex was build using ideal A-form double helical model. the Tpy metallic coordination was constrained using literature data [16].

References

[1] R. T. Batey, R. P. Rambo, J. A. Doudna, *Angew. Chem. Int. Ed.* **1999**, *38*, 2327

[2] J. J. Toulmé, C. Di Primo, S. Moreau, *Prog. Nucleic Acid Res. Mol. Biol.* **2001**, *69*, 1

[3] P. Svoboda, A. D. Cara, *Cell Mol. Life Sci.* **2006**, 63, 901

[4] J. L. Mergny, L. Lacroix, *Oligonucleotides* **2003**, *13*, 515

[5] C. Dietrich-Buchecker, J. Sauvage, *Chem. Rev.* **1987**, *87*, 795

[6] F. Vögtle, T. Dünnwald, T. Schmidt, *Acc. Chem. Res* **1996**, *29*, 451

[7] G. R. Newkome, T. J. Cho, C. N. Moorefield, P. P. Mohapatra, L. A. Godinez, *Chem. Eur. J.* **2004**, *10*, 1493

[8] H. Hofmeier, R. Hoogenboom, M. E. Wouters, U. S. Schubert, *J. Am. Chem. Soc.* **2005**, *127*, 2913

[9] J. Sauvage, J. Collin, J. Chambron, S. Gillerez, C. Coudret, *Chem. Rev.* **1994**, *94*, 993

[10] J. M. Berg, Y. Shi, *Science* **1996**, *271*, 1081

[11] R. Hogg, R. Wilkins, *J. Chem. Soc.* **1962**, , 341

[12] L. Zapata, K. Bathany, J. M. Schmitter, S. Moreau, *Eur. J. Org. Chem.* **2003**, *6*, 1022

[13] A. V. Pisarev, N. E. Shirokikh, C. U. Hellen, *C. R. Biol.* **2005**, *328*, 589

[14] F. Freville, N. Pierre, S. Moreau, *Can. J. Chem.* **2006**, *84*, 854

[15] N. N. Dioubankova, A. D. Malakhov, D. A. Stetsenko, V. A. Korshun, M. J. Gait, *Org. Lett.* **2002**, *4*, 4607

[16] A. T. Baker, H. A. Goodwin, *Aust. J. Chem.* **1985**, *38*, 207

[17] R. Holyer, C. Hubbard, S. Kettle, R. Wilkins, *Inorg. Chem.* **1966**, *5*, 622

[18] M. Goritz, R. Kramer, *J. Am. Chem. Soc.* **2005**, *127*, 18016

[19] M. Egli, *Angew. Chem. Int. Ed.* **1996**, *35*, 1894

[20] D. Lilley, *Biopolymers* **1998**, *48*, 101

[21] P. B. Moore, *Annu. Rev. Biochem.* **1999**, *68*, 287

[22] D. Wemmer, in 'Nucleic Acids, Structures, Properties And Functions', Ed. V. Bloomfield, D. Crothers, I. Tinoco, Sausalito, 1999, , p.111

[23] J. Feigon, W. A. Denny, W. Leupin, D. R. Kearns, *J. Med. Chem.* **1984**, *27*, 450

[24] W. D. Wilson, F. A. Tanious, R. A. Watson, H. J. Barton, A. Strekowska, D. B. Harden, L. Strekowski, *Biochemistry* **1989**, *28*, 1984

[25] D. Collin, C. Heijenoort, C. Boiziau, J. Toulme, E. Guittet, *Nucleic Acids Res.* **2000**, *28*, 3386

Table 1

Strand number																Calcd. Isotopic Mass	Exp. $[M-H]^-$
1	5'	G	G	T	C	C	T	T	T	C	T	T	G	G		3'		
1r	5'	G	G	U	C	C	U	U	U	C	U	U	G	G		3'		
2	5'				C	C	T	T	T	C	T	T	G			3'		
2r	5'				C	C	U	U	U	C	U	U	G			3'		
3	5'				C	A	A	G	A	A	A	G	G			3'		
3m	5'				C	A	A	G	A	A	A	G	G			3'		
4	5'				C	A	A	A	A	A	A	G	G			3'		
5	5'				C	A	A	G	A	A	A	G	G	P		3'	3362.76	3361.75
5m	5'				C	A	A	G	A	A	A	G	G	P		3'	3632.85	3631.84
6	5'			P	C	A	A	G	A	A	A	G	G			3'	3362.76	3361.75
7	5'			P	C	A	A	G	A	A	A	G	G	P		3'	3945.98	3944.95
7m	5'			P	C	A	A	G	A	A	A	G	G	P		3'	4216.07	4215.06
8	5'			P	C	A	A	G	A	A	A	G	G	T	P	3'	4250.02	*4249.00*
8m	5'			P	C	A	A	G	A	A	A	G	G	U	P	3'	4536.11	4535.09
9	5'		P	T	C	A	A	G	A	A	A	G	G	T	P	3'	4554.07	4553.04
9m	5'		P	T	C	A	A	G	A	A	A	G	G	T	P	3'	4824.16	4823.21

Table 2

Duplexes	Strands	Metal free buffer	Zn^{2+} 1 eq.	Fe^{2+} 1eq.	Ni^{2+} 1eq.	Zn^{2+} 20 eq.	Fe^{2+} 100 eq.	Ni^{2+} 2 eq.
0a	1,3	28.9	28.3	29.5	nd			
0b	1,4	n	n					
Ia	1,5	31.2	31.6	32.3				
Ib	1,6	33.5	34.6	35.0				
IIa	1,7	35.1	10~20	10~20	10~20	28.3	10~20	42.4
IIb	1,8	35.0	10~20	10~20	10~20			
IIc	1,9	34.2	10~20	10~20	10~20			
0c	2,3	26.5	24.9	26.4				
Ic	2,5	29.1	30.4	29.0				
Id	2,6	33.4	33.6	32.9				
IId	2,7	34.0	10~20	10~20			10~20	36.4
IIe	2,8	32.8	10~20	10~20	10~20		10~20	36.6
IIf	2,9	32.6	10~20	10~20			10~20	36.1

Table 3

Duplexes	Strands	Metal free buffer	Zn^{2+} 1 eq.	Fe^{2+} 1eq.	Ni^{2+} 1eq.	. Ni^{2+} 2 eq.	Zn^{2+},1 eq. Mg^{2+} (3mM) .	Zn^{2+},1 eq. Mg^{2+} (10mM)
0ra	1r,3m	40.4	40.3	40.6			40.0	41.8
Ira	1r,5m	41.4	42.2	41.7				
IIra	1r,7m	43.3	29.9	29.4	31.4	39.8	33.5	42.8
IIrb	1r,8m	44.6	33.2	36.2	35.0	43.1	39.0	44.3
IIrc	1r,9m	43.3	37.3	37.1	35.7	41.2	42.4	46.6

Table 4

Strand Number	***Species***	***Calculated Data***	***Experimental***
5	$[M-H]^-$	3361.75	3361.75
5 + Fe	$[2M+Fe-3H]^-$ $[2M+Fe-4H]^{2-}$	6778.34 3388.67	6778.27 3388.60
5m + Fe	$[2M+Fe-3H]^-$ $[2M+Fe-4H]^{2-}$	7318.61 3658.80	7318.55 3658.79
7	$[M-H]^-$	3944.98	3944.95
7 + Fe	$[M+Fe-3H]^-$	3998.89	3998.91
7m	$[M-H]^-$	4215.07	4215.09
7m + Fe	$[M+Fe-3H]^-$	4268.98	4268.99
2+7+Zn	$[M_2-H]^-$ $[M_7+Zn-3H]^-$ $[M_7+2Zn-5H]^-$ $[M_{IIId}+Zn-3H]^-$ $[M_{IIId}+2Zn-5H]^-$	2653.46 4006.89 4068.81 6666.14 6728.06	2653.45 4006.87 4068.79 6666.00 6729.00
2+7+Ni	$[M_2-H]^-$ $[M_7+Ni-3H]^-$ $[M_7+2Ni-5H]^-$ $[M_{IIId}+Ni-3H]^-$ $[M_{IIId}+2Ni-5H]^-$	2653.46 4000.89 4056.81 6659.44 6716.11	2653.46 4000.87 4056.81 6659.00 6716.00

Table 5

				1	2	3	4	5	6	7	8	9		
5'	G	G	T	*C*	C	T	T	T	C	T	T	*G*	G	3'
3'				*G*	G	A	A	A	G	A	A	*C*		5'

	Imino protons								
	G1	G2	T3	T4	T5	G6	T7	T8	G9
Duplexes									
0a	12.58 a	12.68	13.97	13.83	13.52	12.09	13.66	13.97	12.41 a
Ia		12.42 (0.26)	13.82 (0.15)	13.75 (0.08)	13.47 (0.05)	12.09	13.66	13.96	
IIa					13.45 (0.07)	12.09 (0)	13.57 (0.1)	13.77 (0.2)	12.11 (0.3)
Ia + Zn		12.43	13.88	13.75	13.47	12.10	13.67	13.96	
IIa + Zn		12.61	13.94	13.77	13.45	12.08			

Legends

Table 1

Sequences of the various strands used in this study. r stands for ribonucleotides, m for 2'-O-Me-ribonucleotides. Mass spectral data were recorded on a Maldi-Q-TOF spectrometer (mass accuracy better than 0.01 Da, see experimental procedure)

Table 2

Melting temperatures of the various DNA duplexes formed from strand association (column 2). Tm (± 1°C) are mean values of at least three experiments. Buffer : 10mM phosphate buffer (pH 7.0) 150 mM NaCl. Metal free buffer was completed with 200 µM EDTA. eq. refers to duplex concentration (1 µM), n stands for no transition, 10~20 stands for Tm between 10 to 20°C

Table 3

Melting temperature of the RNA duplexes formed from the strand associations shown in column 2. Tm (± 1°C) are mean values of at least three experiments. Buffer : 10mM phosphate buffer (pH 7.0) 150 mM NaCl. Metal free buffer was completed with 200 µM EDTA. eq. refers to duplex concentration (1µM).

Table 4

Mass spectral data of oligonucleotide strands and duplexes. MALDI-Q-TOF mass spectrometry was performed on a Waters Ultima spectrometer (see experimental procedure for details on

sample preparation). Mass accuracy better than 0.01 Da.

Table 5

The chemical shifts (ppm) of the imino proton resonances in the various duplexes.

a: reversible assignments.

In parentheses ΔTm = Tm(duplex 0a) - Tm(duplex **Ia** or **IIa**)

Figure 1

UV melting curves (260 nm) of duplexes **0a** (links) and **IIa** (right). Concentration of duplexes 1µM, in the presence of one equivalent of Zn^{2+} ions (1µM). The heating rate was 0.5°C/min,. Y axis (%H) is the percent of hyperchromicity.

Figure 2

MALDI-Q-TOF spectra of strand **7** after metalation with Fe^{2+}. Inset : isotopic distribution of the main species $[M_7+Fe-3H]^-$

Figure 3

Denaturating 20 % PAGE analysis. A) Visualization by UV shadowing. Lane 1(1r); lane 2 (**5m**); lane 3 (**7m**); lane 4 (**7m** + Fe^{2+}); lane 5 (**5m** + Fe^{2+}); lane 6 (**2m**). B) Same gel visualized under daylight. Lanes 4', 5', correspond to lanes of 4, 5, (Figure 3A). Purple coloured spot lane 4' and 5' revealed Iron II Tpy complexes.

Figure 4

One-dimensional 1H NMR spectra of the exchangeable imno region (11-15 ppm) of the various

duplexes. 4A duplex **0a**, 4B duplex **Ia**, 4C duplex **IIa**, 4D duplex **Ia** with one equivalent of Zn^{2+} ions, 4E duplex **IIa** with one equivalent of Zn^{2+} ions. Base pair numbers are indicated in the included sketch upper right. Imino protons are numbered accordingly.

eq. refers to duplex concentration (1 µM), n stands for no transition.

Figure 5

Expanded imino-imino region of the two dimensional NOESY map in 90/10 H2O/D2O for the duplex **0a**. The lines illustrate the NOE walk along the imino protons. Imino proton are numbered according to base pair numbers.

Scheme 1

Schematic representation of a catenane structure (A). Cyclisation of a bis(Tpy) modified oligonucleotide on a target strand upon metal chelation

Scheme 2

Chemical structure of bis(Tpy) conjugated oligonucleotides (A). Optimized structure of a A-form duplex with constrained Tpy distances. (see experimental part).

Scheme 1

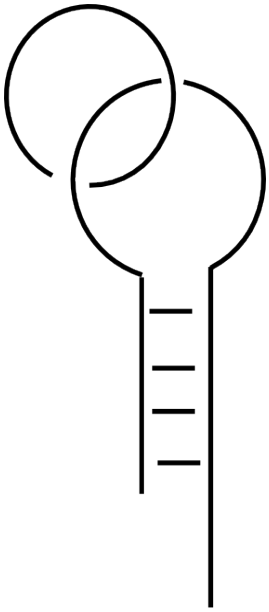

A

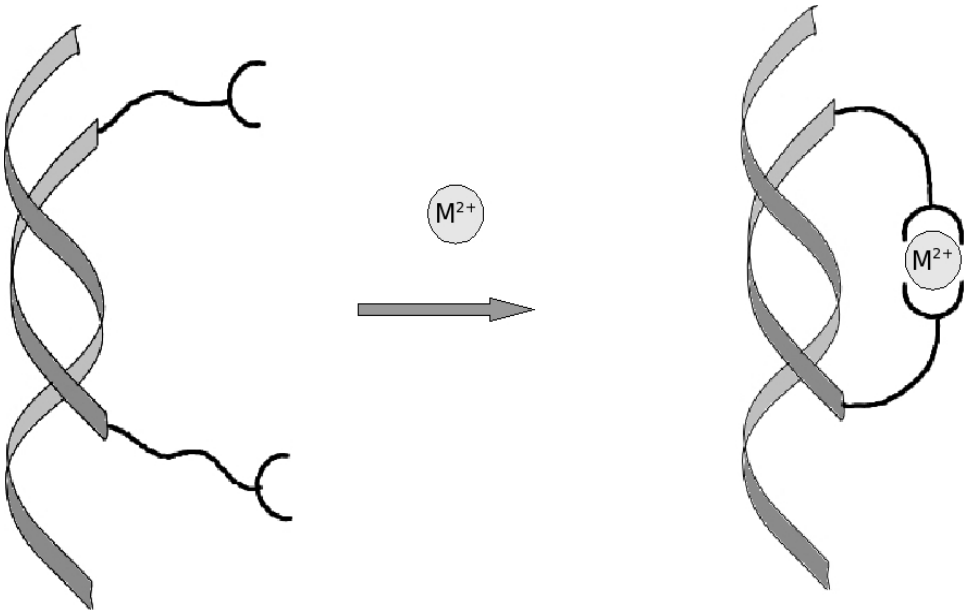

B

Scheme 2

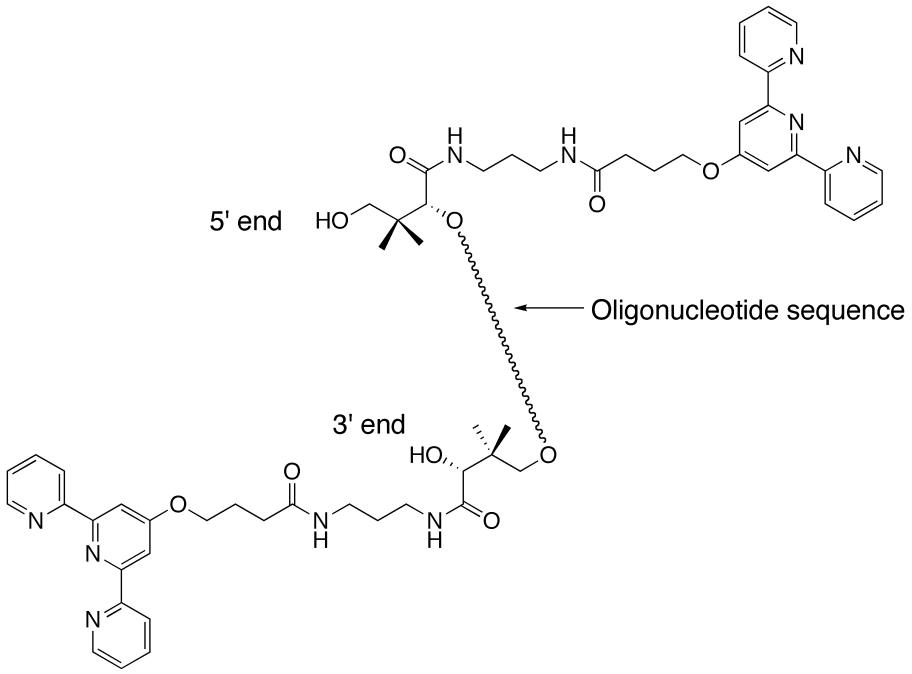

A

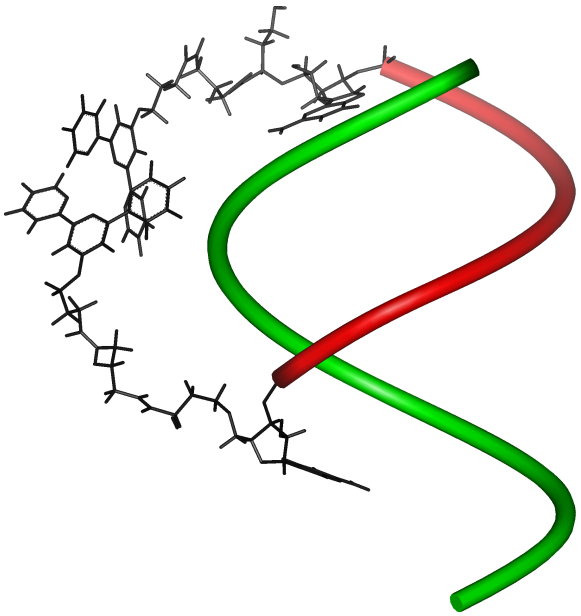

B

Figure 1

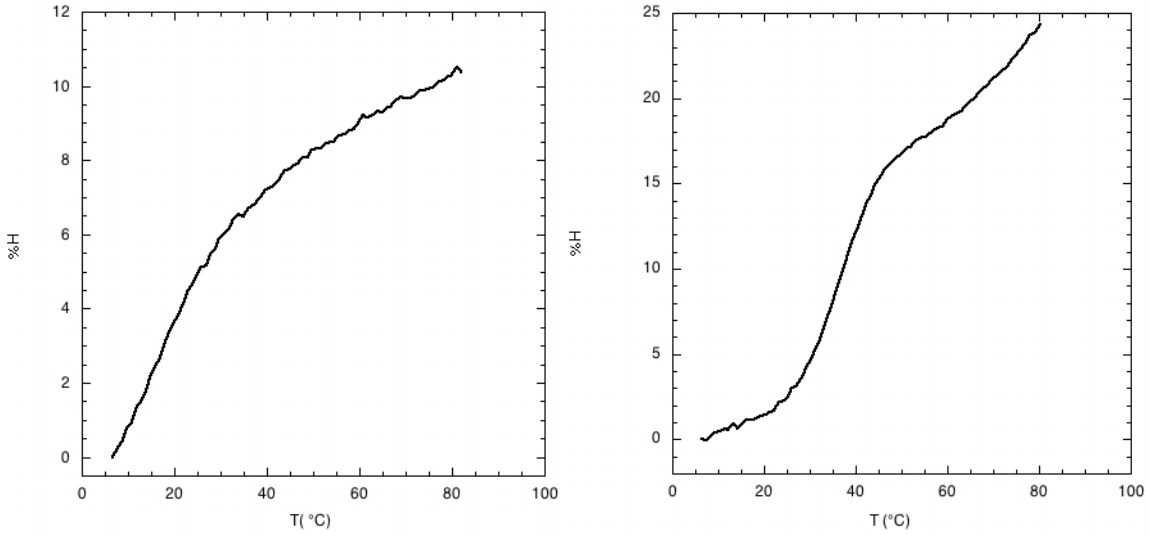

0A IIa

Figure 2

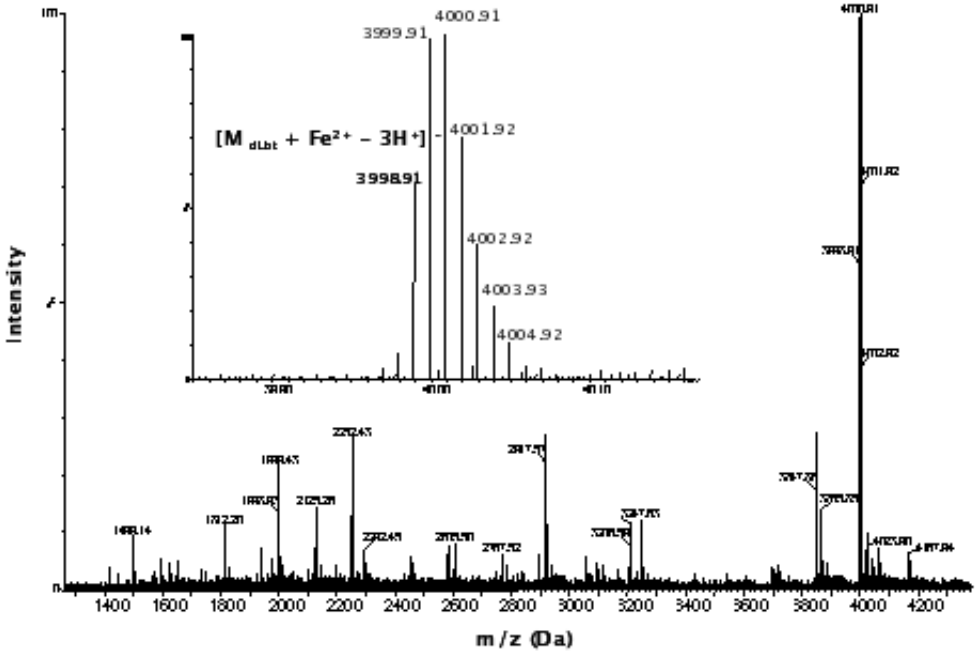

Figure 3

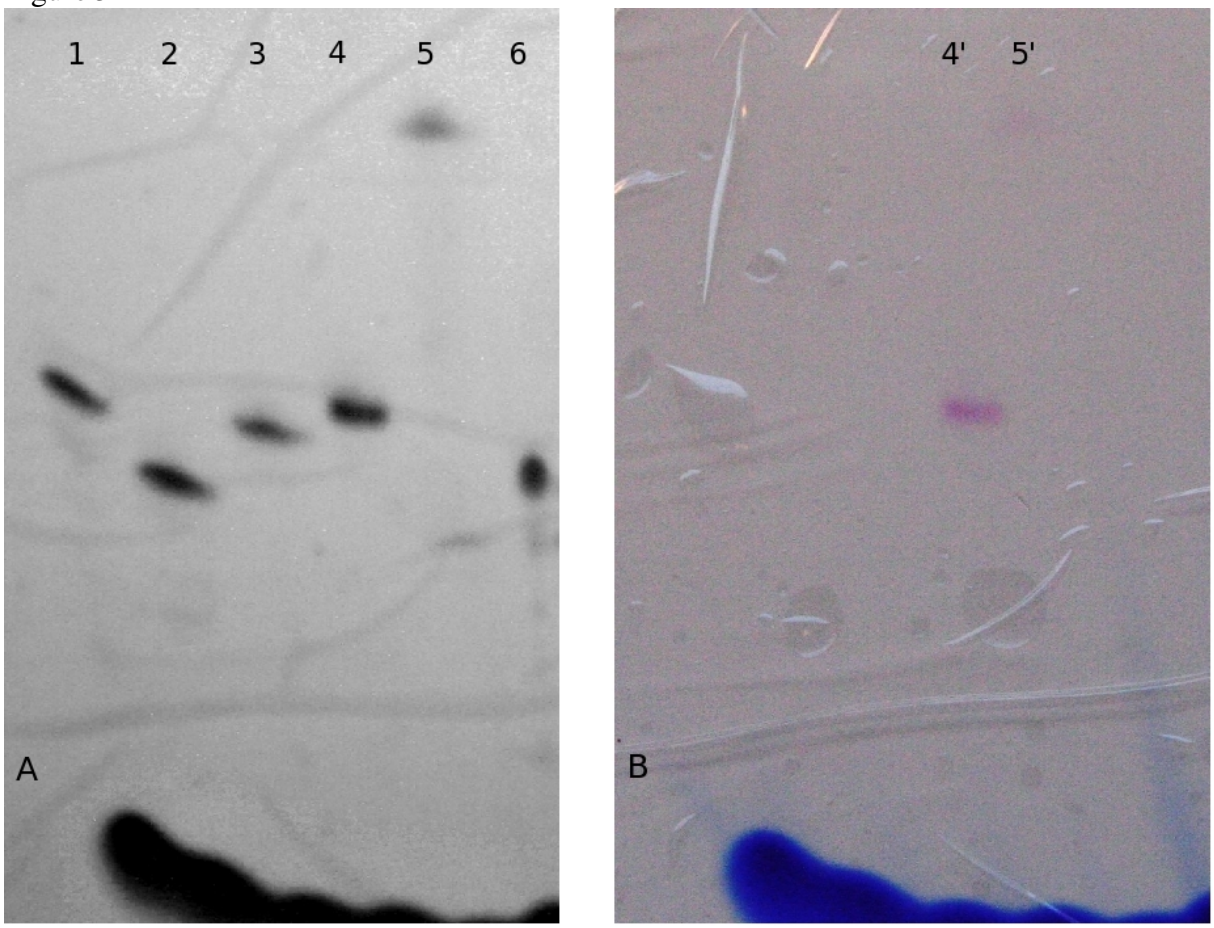

Figure 4

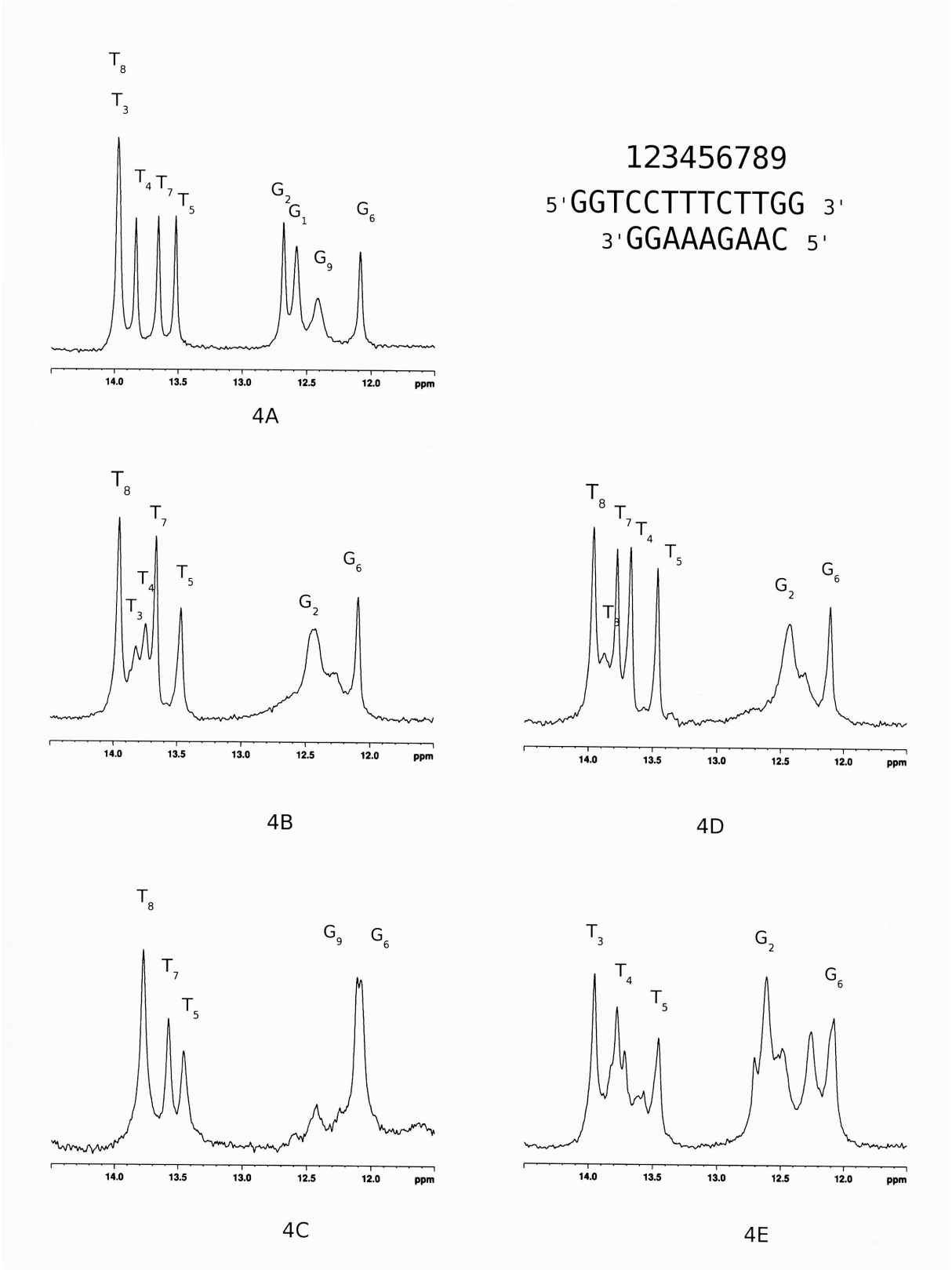

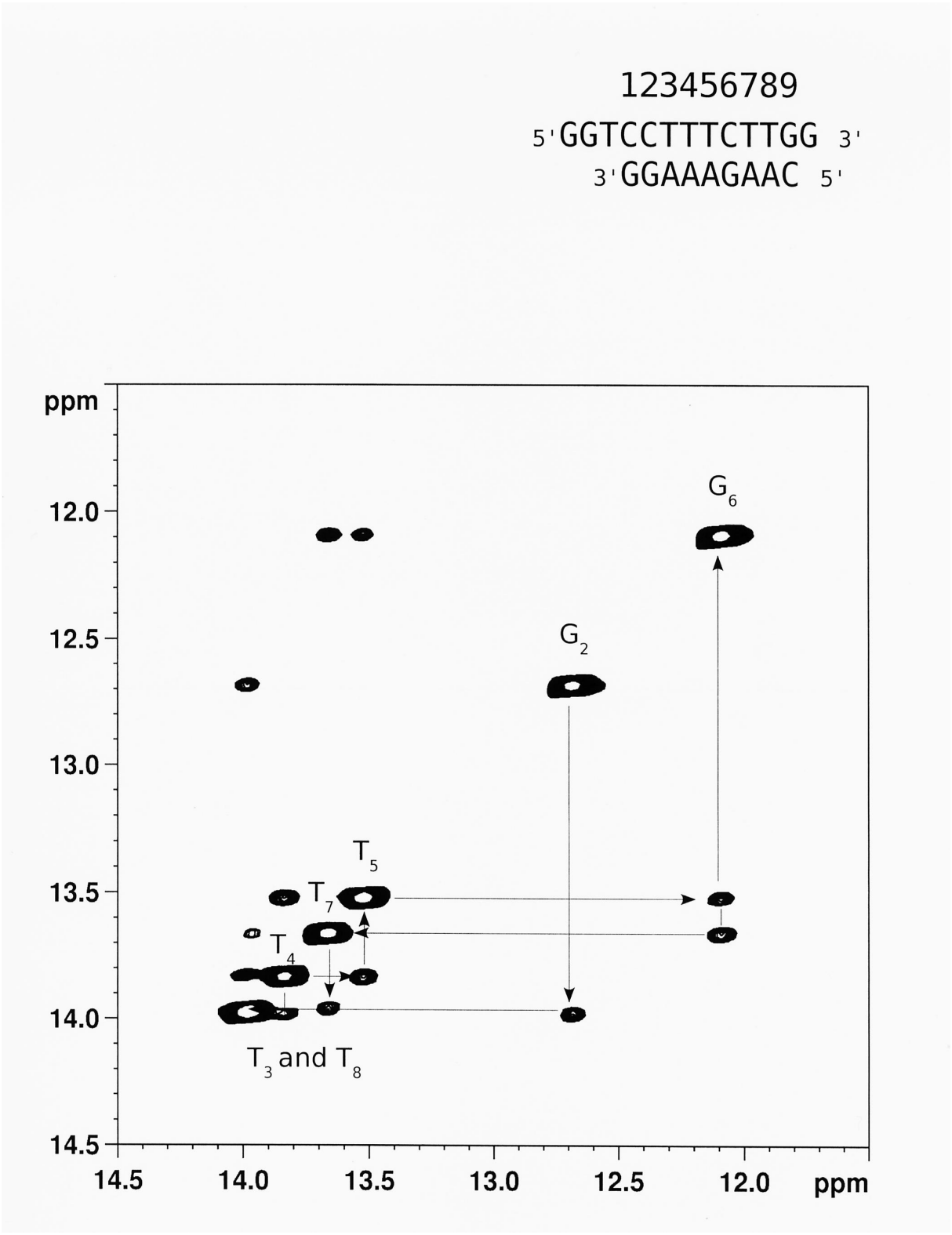

Table of Contents

Conjugation of chelating 2,2':6',2"-terpyridine moieties at both 3' and 5' ends of oligonucleotides allowed a smooth cyclization of this oligomer on its complementary target upon addition of metal ion.